01

Heat balance method of computing the cooling modes of large-sized optics in vacuum

© A.V. Zavatskaya, Yu.A. Rezunkov

„Scientific Research Institute for Optoelectronic Instrument Engineering, Sosnovy Bor, Leningrad region, Russia
e-mail: yuri@sbor.net

Received November 24, 2022
Revised February 7, 2023
Accepted February 14, 2023

The heat balance method is developed to optimize cooling modes of large-sized optics in a special cryogenic-vacuum system by considering a complicated heat transfer in the system to minimize the optics thermal deformations.

Keywords: radiative heat transfer, conductive heat transfer, heat balance, thermostat, collimator.

DOI: 10.21883/TP.2023.05.56061.253-22

Introduction

A necessary stage in the development of advanced infrared optoelectronic equipment (IR OEA) is the testing of its spatial and energy resolution in vacuum conditions. The tests of the IC OEA are conducted with a low temperature background due to the cooling of the optical equipment that is part of the thermal vacuum test bench [1–3]. An important element of this equipment is an optical collimator that matches the fields of view of the test device and the test equipment. When the collimator is cooled from room to cryogenic temperatures, it is necessary to prevent the possibility of thermal deformations of its elements affecting the optical quality (alignment) of the collimator. It was proposed in [4],to cool the collimator through the heat exchange using radiation of optical elements with special cryogenic screens installed in the vacuum chamber of the test bench. At the same time, the method of thermal balance provided in a stationary state by radiation heat exchange of large-sized optics with a thermostat was used to calculate the cooling modes.

ANSYS software can be used for calculation of complex heat exchange by radiation inside a closed thermophysical system consisting of individual elements with different physical characteristics [5]. In this case, a stationary solution of non-stationary heat conductivity equations is found for each element of the system with boundary conditions defined using the thermal balance method [6]. In the balance method — these are equations relating the resulting radiation flux and the temperature of each surface to the heat fluxes from the other surfaces. In general form, the heat balance equation for the kth surface has the following form:

$$\sum_{j-1}^{N}\left(\delta_{kj}-\varphi_{kj}\frac{1-\varepsilon_j}{\varepsilon_j}\right)\frac{Q_j}{F_j}=\sum_{j=1}^{N}(\delta_{kj}-\varphi_{kj})\sigma T_j^4, \quad (1)$$

where Q_j — the resulting heat flow from the surface j; T_j — temperature of jth surface; F_j — area of jth surface; ε_j — the degree of blackness of the surface; φ_{kj} — the angular coefficient of heat transfer between the surfaces k and j; σ_0 — Stefan–Boltzmann constant, $5.67\cdot10^{-8}\,\mathrm{W/(m^2K^4)}$; σk_j — Kronecker symbol. The index k corresponds to the selected surface, and the index j corresponds to other surfaces of the closed region.

However, the sequential solution of non-stationary equations, when it is necessary to construct complex computational grids, leads to a significant increase in the computing time in the ANSYS software. Nevertheless, the solution obtained depends both on the correctness of the formulated thermophysical model of the cooling process and on the accuracy of calculation of the angular coefficients of heat exchange by radiation.

This paper considers the generalization of the heat balance method we proposed earlier for the case of thermal equilibrium inside a closed system „collimator primary mirror (CPM)–thermostat–vacuum chamber“, when both heat exchange by radiation and conductive heat exchange due to the thermal conductivity of the materials of the cooled elements are taken into account.

The conductive heat transfer is taken into account in the proposed method without involving non-stationary heat conduction equations. This reduces the computing time and allows for a relatively fast optimization of both the structure of the thermostat and the cooling modes of the optics, depending on many structural and thermophysical parameters of the elements of the thermophysical system. The method of successive approximations is used to solve the system of nonlinear algebraic equations of thermal balance formed in this case similar to Newton's method and implemented in the Mathcad program.

The thermal balance method also makes it possible to estimate temperature gradients in the elements of large-sized optics when they are cooled under thermal vacuum conditions. The optimal cooling mode is considered to be one in which the minimum temperature gradients in

the optical elements are provided, determined by the requirement to preserve the optical quality of the collimator.

The convergence of the method is controlled by the initial heat balance equations, when the temperature values obtained at each iteration step are inserted in them. The thermal balance conditions of each element were observed with an accuracy of up to 10^{-8} W.

1. Thermophysical model of a thermovacuum cooling system and temperature stabilization of the thermostat type

The developed structure of the large-sized optics cooling system under vacuum conditions — thermostat is shown in Fig. 1 [4]. Its design comprises a set of cryo-screens (i.e., special screens cooled by an external cryosystem) and heat shields jointly located inside a cylindrical vacuum chamber. It is necessary to keep the spatial volume free within the angular field of view of the collimator and the tested equipment due to the peculiarities of the construction of optical systems of the collimator and the conditions of testing of the infrared optical-electronic equipment. This is achieved by using cryo-screens and cylindrical heat shields.

Three groups of thermophysical objects can be distinguished in the thermostat, namely:

— heat sources, i.e., walls of the vacuum chamber *9*, and drains, i.e., cryo-screens *2, 3* with individual cooling;

— heat-protective metal screens *4*–*7* with screen-vacuum thermal insulation (SVTI);

— the cooled elements of the collimator (in this case, the main mirror of the collimator *1* and the stand *8*).

The cooling of the CPM to a set temperature T_1 is carried out due to heat exchange by radiation between the mirror and cylindrical cryo-screens on both sides with independent control of their temperature (T_2, T_3). The geometric dimensions of the cryo-screens are selected so that they ensure maximum efficiency of heat exchange between the mirror and the screens. The temperature of

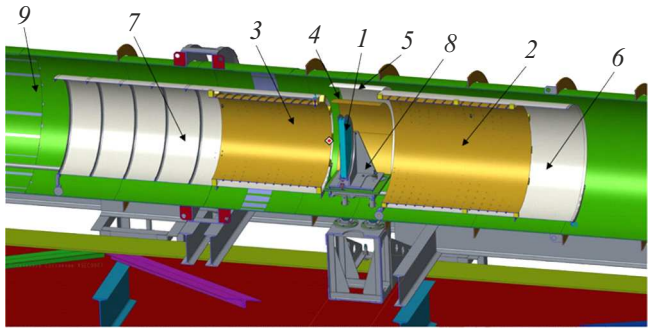

Figure 1. The block diagram of the thermostat combined with the CPM: *1* — the main mirror of the collimator, *2, 3* — cylindrical cryo-screens, *4*–*7* — heat shields, *8* — mirror stand, *9* — walls of the vacuum chamber.

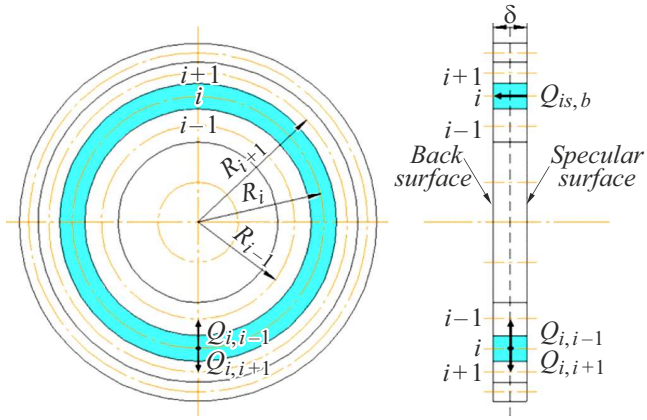

Figure 2. Scheme for calculating the conductive heat exchange of local zones in the axial and radial directions along the mirror.

the walls of the vacuum chamber T_9 is considered constant and equal to the ambient temperature.

Due to the design features, the heat exchange by radiation between the parts of the thermostat (left and right of the CPM) separated by a mirror is very limited. Therefore, the thermal balance inside the thermostat will also depend on the conductive heat exchange between the corresponding surfaces of the CPM. The back and mirror surfaces of the mirror have different degrees of blackness, which leads to an asymmetry in the efficiency of the heat exchange of the mirror with cryo-screens. It should also be borne in mind that individual elements, such as a mirror and a stand under it, are in direct thermal contact, which leads to the need to take into account additional heat flow between these elements. It should also be noted that part of the heat flow from the walls of the vacuum chamber located outside the heat shields falls on the mirror.

To calculate the radial distribution of temperature in the CPM the mirror is conditionally divided into several axisymmetric radial zones (Fig. 2) for each of which the heat balance equation is written with the corresponding angular coefficients of radiant heat transfer. We consider a steady-state thermal balance regime with a stationary temperature distribution in each element. This distribution is linear from one surface (rear) to another (mirror) for a cooled mirror, which can be considered as a flat plate with a small thickness-to-diameter ratio since there are no additional heat sources inside the mirror. The temperature distribution in the annular radial zone, into which the mirror is divided along its radius, is also linear. The heat flow between the adjacent surfaces of each zone arises due to the thermal conductivity of the mirror material and affects the conditions of the thermal balance of each zone.

The conditions of heat exchange by radiation with a heat shield located around the mirror are set for the outer (end) surface of the mirror.

Below, as an example, the heat balance equation for the mirror surface of the i-th zone of the CPM is given in

general form:

$$\sum_{\substack{j=1\\ j\neq k}}^{N}\varepsilon_{ij}\sigma_0\phi_{ij}f_i\left(T_j^4-T_j^4\right)+\frac{\lambda}{\delta_i}F_i(T_{i,s}-T_{i,b})+\frac{\lambda}{(R_{i+1}-R_i)}$$
$$\times F_{i\text{ext}}\left(\frac{T_{i,s}+T_{i,b}}{2}-\frac{T_{i+1,s}+T_{i+1,b}}{2}\right)+\frac{\lambda}{(R_i-R_{i-1})}$$
$$\times F_{i\text{int}}\left(\frac{T_{i,s}+T_{i,b}}{2}-\frac{T_{i-1,s}+T_{i-1,b}}{2}\right)=0, \tag{2}$$

where ε_{ij} — reduced degree of blackness between the surfaces of interacting elements; σ_0 —Stefan–Boltzmann constant, $5.67\cdot10^{-8}$ W/(m^{2}K^4); φ_{ij} — angular coefficient of radiation between surfaces; F_i — surface area of the ith element of the CPM; $F_{i\text{ext}}$ — area of the outer end surface ith of the CPM element; $F_{i\text{int}}$ — area of the inner end surface ith of the CPM element; λ_i — reduced thermal conductivity coefficient of the CPM material; δ_i — thickness of the ith element; $T_{i,s}$ — temperature of the mirror surface of the ith radial zone of the CPM; $T_{i,b}$ — temperature of the back surface of the ith radial zone of the CPM; $T_{i+1,s}$ — temperature of the mirror surface of the $i+1$th radial zone of the CPM; $T_{i+1,b}$ — temperature of the back surface of the $i+1$th radial zone of the CPM, $T_{i-1,s}$ — temperature of the mirror surface of the $i-1$th radial zone of the CPM, $T_{i,b}$ — the temperature of the back surface of the $i-1$th radial zone of the CPM.

The reduced degree of blackness is determined in terms of angular coefficients as follows [7]:

$$\varepsilon_{ij}=\frac{1}{1+\varphi_{ij}\left(\frac{1}{\varepsilon_i}-1\right)+\varphi_{ji}\left(\frac{1}{\varepsilon_j}-1\right)},\quad \varphi_{ji}=\frac{F_i}{F_j}\varphi_{ij}, \tag{3}$$

where ε_i and ε_j — degrees of blackness of two interacting surfaces.

Similarly, the heat balance equations are written for the surfaces of each ith element of the system „CPM–thermostat–vacuum chamber“, which are involved in radiation heat exchange with the surfaces of the elements of this section, as well as in conductive heat exchange between by myself.

2. Method for calculating temperature parameters under conditions of thermal balance of the system „CPM–thermostat–vacuum chamber“

The conditions of the thermal balance of the system „CPM–thermostat–vacuum chamber“are described by a system of nonlinear algebraic equations based on (2) and (3) relatively unknown temperature parameters of cooled optics elements and heat shields. The cooling modes are controlled by cryo-screens, the temperature parameters of which are also included in these equations. The calculation of the cooling mode of the CPM is reduced to finding such values of the temperature of the cryo-screens at which the mirror is cooled to a predetermined temperature. The optimal mode is considered to be one that provides minimal temperature gradients in the optical elements that occur during cooling.

The method of successive approximations is used to solve the resulting system of nonlinear algebraic equations with a preliminary transformation of unknown temperature parameters to the form of variations relative to the temperature values of cryo-screens. These transformations for each individual part of the thermostat are as follows: $\delta T_i=T_i-T_2$ for the right part of the thermostat and $\delta T_j=T_j-T_3$ for the left part. Accordingly, both radiation (4), i.e. due to heat exchange by radiation, and conductive (5) terms are transformed:

$$T_i^4-T_j^4=(T_i-T_j)(T_i+T_j)(T_i^2+T_j^2)$$
$$=(\delta T_i-\delta T_j)(T_i^2+T_j^2)(T_i+T_j), \tag{4}$$

$$\frac{\lambda_i}{\delta_i}(T_{ik}-T_{i,k+1})=\frac{\lambda_i}{\delta_i}(\delta T_{i,k}-\delta T_{i,k+1}+\Delta T_{2,3}). \tag{5}$$

Then, by converting the equation (2) to a linear form with respect to the variations T_i, we obtain

$$(P_i+J_i+Q_i+R_i+S_i)\delta T_{i,s}+Q_i\delta T_{i_1,s}+R_i\delta T_{i-1,s}$$
$$+(Q_i-J_i+R_i)\delta T_{i,b}+Q_i\delta T_{i+1,b}+R_i\delta T_{i-1,b}-P_i\delta T_j$$
$$=S_i\Delta T_{92}-J_i\Delta T_{23}, \tag{6}$$

where

$$P_i=\sum_{\substack{j=1\\ j\neq i}}^{N}\varepsilon_{ij}\sigma_0\phi_{ij}F_i(T_i+T_j)(T_i^2+T_j^2),\quad J_i=\frac{\lambda_i}{\delta_i}F_i,$$

$$Q_i=\frac{\lambda_i}{2(r_{i+1}-R_i)}F_{i\text{ext}},\quad R_i=\frac{\lambda_i}{2(R_i-R_{i-1})}F_{i\text{int}},$$
$$S_i=\varepsilon_{i9}\sigma_0\phi_{i9}F_i(T_i+T_9)(T_i^2+T_9^2)$$

the heat transfer coefficients of radiation heat exchange and conductive heat exchange that have dimension [W/K]. $\delta T_{i,s}=T_{i,s}-T_2$, $\delta T_{i+1,s}-T_2$, $\delta T_{i-1,s}=T_{i-1,s}-T_2$, $\delta T_j=T_j-T_2$, $\delta T_{i,b}=T_{i,b}-T_3$, $\delta T_{i+1,b}=T_{i+1,b}-T_3$, $\delta T_{i-1,b}=T_{i-1b}-T_3$, $\Delta T_{23}=T_2-T_3$, $\Delta T_{92}=T_9-T_2$ — temperature variations of the elements of the thermovacuum system relative to the temperatures of cryo-screens with a dimension of [K].

At the same time, additional terms with $\Delta T_{23}=T_2-T_3$, $\Delta T_{92}=T_9-T_2$ appear in the transformed equations. $\Delta T_{93}=T_9-T_3$ appears in the last term instead of ΔT_{92} for the back surface. The difference in the temperature values of the cryo-screens, as well as the temperature of these screens with the temperature of the walls of the vacuum chamber, determine the final conditions of the thermal balance in the thermostat.

The equations for the other elements of the thermostat are written in the same way. There are terms in each equation of type (6) that depend both on the temperature of specific elements involved in heat exchange and on their thermophysical characteristics, namely, on the degree of blackness of the surface and the thermal conductivity of the material of the elements.

It should be noted that the equations (6) express the thermal equilibrium of the cooling system under consideration based on the general differential principles of temperature change of its constituent elements relative to the specified temperature parameters of cryo-screens [8]. The optimal cooling mode of the mirror, when the temperature gradients in it are within the tolerance set by the requirements for the optical system of the collimator, is chosen based on nomograms of the isotherms of the thermal state of the CPM, composed as functions of the mirror temperature T_2 and temperature gradients in it from T_2 and T_3.

The resulting system of equations is solved by the well-known Gauss method with respect to δT in MathCAD with the conditions of convergence of this method. The convergence of the method of successive approximations is given by the necessary condition that the main determinant of the coefficient matrix of a system of equations of type (6) is not equal to zero. The rule $T_i^n - T_i^{n-1} \leq \xi$ is used as a condition for the end of iterations in calculations. Here n is the iteration number, ξ is the calculation error. $\varepsilon = 10^{-5}$ was set in calculations. The obtained solution were verified using the initial equations (2) after substituting the obtained temperature values of all elements in them. At the same time, the value of the thermal imbalance in each equation did not exceed 10^{-8} W.

3. Cooling modes of large-sized optics (the main mirror of the collimator) in the thermostat

The important parameters in the equations (2) are the angular coefficients of heat exchange by radiation φ_{ij} between the elements of the system „CPM–thermostat–vacuum chamber“. An algebraic method was used [6] to calculate specific values of φ_{ij} between surfaces of different shapes (for example, mirrors and cylindrical screens) which allows generalizing analytical expressions of simple special cases to more complex configurations of interacting surfaces.

The calculation of angular coefficients of heat exchange by radiation using the algebra of angular coefficients makes it possible to significantly simplify the analysis of the results of thermal calculations to optimize the cooling system. The magnitude of the angular coefficients, in addition to determining the accuracy of the results of the thermal calculation, also makes it possible to assess the mutual influence of the system elements on each other, on the thermal balance, on the average temperature of the cooled element and temperature gradients in it.

For example, consider the heat exchange by radiation between two end surfaces F_i and F_m, where F_i is the disk, F_m is the inner surface of the cylinder (Fig. 3), which denote the surfaces of the CPM and the inner surface of the walls of the vacuum chamber. All surfaces of elements in a closed system „CPM–thermostat–vacuum chamber“ in the subject thermophysical model are considered diffuse gray.

We write

$$\phi_{m,i} = \phi_{m,i+j} - \phi_{m,j}.$$

using the algebra of angular emission coefficients

It is possible to use the calculated formula of the angular coefficient between the inner surface of the straight cylinder and the disk at its base to determine $\varphi_{m,i+j}$ and $\varphi_{m,j}$ [9]. To do this, extend the surface m to the intersection with the surface plane i. We get an additional conditional surface n.

Based on the algebra of angular coefficients, [6] the following is valid:

$$F_{m+n} = F_m + F_n \quad \text{and} \quad F_{i+j} = F_i + F_j,$$

$$F_{m+n}\varphi_{=}F_m\varphi_{m,j} + F_m\varphi_{n,j},$$

$$F_{m+n}\varphi_{m+n,i+j} = F_m\varphi_{m,i+j} + F_n\varphi_{n,i+j},$$

where F_{m+n} is the total surface area m and n, F_n is the area of imaginary cylindrical surface n, F_i is the surface area of the ring.

Then

$$\varphi_{m,i+j} = \frac{F_{m+n}\varphi_{m+n,i+j} - F_n\varphi_{n,i+j}}{F_m},$$

$$\phi_{m,j} = \frac{F_{m+n}\phi_{m+nj} - F_n\phi_{n,j}}{F_m}.$$

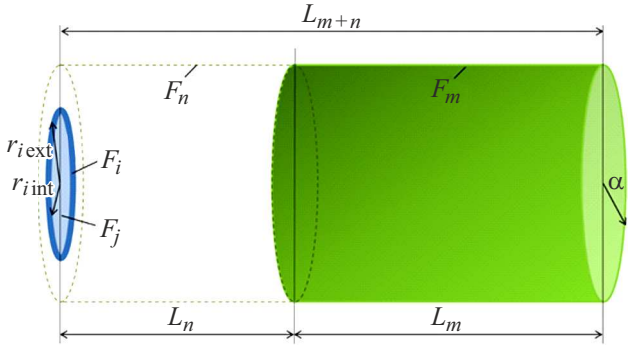

Figure 3. A diagram illustrating the application of an algebraic method for determining the angular coefficient $\varphi_{m,i}$.

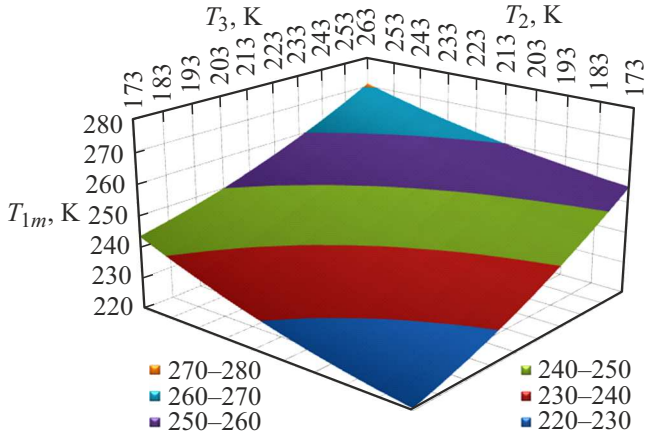

Figure 4. The dependence of the temperature of the central zone of the mirror surface of the CPM T_{1m} on the temperature of the cryo-screens T_2 and T_3.

After a series of transformations for the desired coefficient $\varphi_{m,i}$ we have

$$\phi_{m,i} = \frac{F_{m+n}\left[\sqrt{L_{m+n}^4+2L_{m+n}^2(a^2+r_{i\text{ext}}^2)+(a^2-r_{i\text{ext}}^2)^2}-\right.}{4aL_{m+n}F_m}$$
$$\left.-(a^2-r_{i\text{ext}}^2)-L_{m+n}^2\right]$$
$$-\frac{F_n\left[\sqrt{L_n^4+2L_n^2(a^2+r_{i\text{ext}}^2)+(a^2-r_{i\text{ext}}^2)^2}-(a^2-r_{j\text{ext}}^2)-L_n^2\right]}{4aL_nF_m}$$
$$-\frac{F_{m+n}\left[\sqrt{L_{m+n}^4+2L_{m+n}^2(a^2+r_{i\text{int}}^2)}-(a^2-r_{i\text{int}}^2)-L_{m+n}^2\right]}{4aL_{m+n}F_m}$$
$$-\frac{\left[\sqrt{L_n^4+2L_n^2(a^2+r_{i\text{int}}^2)^2-(a^2-r_{i\text{int}}^2)^2}-(a^2-r_{i\text{int}}^2)-L_n^2\right]}{4aL_nF_m}, \quad (7)$$

where L_{m+n} is the cylinder height F_{m+n}, a is the cylinder radius F_{m+n}, $r_{i\text{ext}}$ is the disk radius F_{i+j}, L_n is the cylinder height F_n, $r_{i\text{int}}$ is the disk radius F_j.

Figure 4 shows the solution of the system of equations (6) in the form of a dependence of the temperature of the mirror surface of the CPM collimator on the temperature of the cryo-screens (T_2 and T_3) for the thermostat parameters specified in [4]. It follows from the figure that the required temperature of the CPM can be achieved with different combinations of cryo-screens temperature values. A corresponding asymmetry of the temperature distribution is observed due to the asymmetry of the thermostat structure relative to the CPM and the degree of blackness of the mirror surfaces, which leads to the appearance of axial temperature gradients in the mirror.

Fig. 5 shows graphs of temperature changes along the radius of the mirror surface of the CPM cooled to a temperature of $T_{1m} = 233$ K, at different temperatures of the cryo-screens T_2 and T_3. We see that the radial temperature distribution in the mirror varies depending on the combination of cryo-screen temperature values. It is possible to determine such temperature values T_2 and T_3 based on the results of calculations, at which the radial temperature drop along the mirror will be minimal.

In particular, it follows from the results of thermal calculations that the temperatures of the screen *4* and the stand *8* determine the radial temperature drop in the mirror. The greater the difference between them and the temperature of the CPM, i.e. ΔT_{8-1}, ΔT_{4-1}, the greater the radial temperature difference in the mirror. The tendency of temperature change from the center to the edge of the CPM also depends on the temperature difference between the mirror and the screen *4*. At $T_4 < T_1$, T_1 decreases from the center to the edge and it increases at $T_4 > T_1$.

specific values of axial and radial temperature differences in the mirror.

The calculation results are presented in the form of nomograms of the isotherms of the CPM to determine the optimal cooling modes, as well as in the form of constant values of the differences in axial and/or radial temperature distributions in it (Fig. 6, 7). In Fig. 6, a nomogram of the temperature parameters of the mirror is shown with the degree of blackness of the heat shield above it $\varepsilon_4 = 0.57$, corresponding to the degree of blackness of the surface of the copper sheet. The picture is provided here in the form of a local icon (blue circle (in online version)) the calculation result of the same thermostat structure in [4]. Note that the result obtained earlier coincides with a more complete picture of the calculation of the thermal state of the CPM system, but with an accuracy of

It also follows from the nomogram on Fig. 6 that the cooling of the CPM to a specific temperature can be provided only in a certain range of temperature changes of

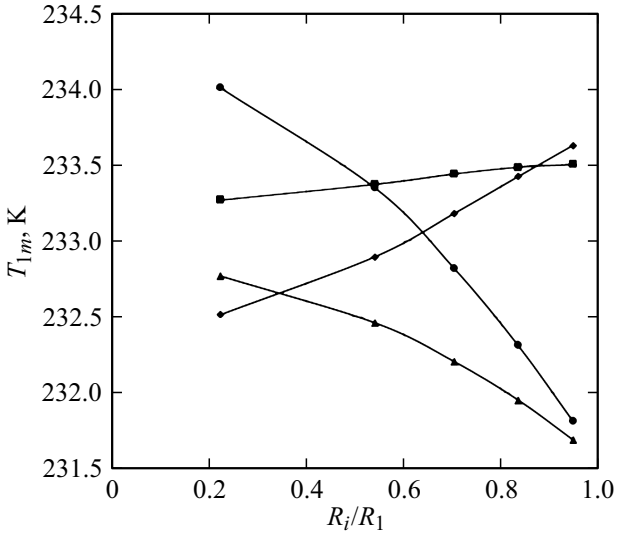

Figure 5. Radial temperature distribution over the mirror surface of the CPM with different values of the temperature of the cryo-screens: –♦– $T_2 = 243$ K, $T_3 = 193$ K; –▲– $T_2 = 210$ K, $T_3 = 210$ K; –■– $T_2 = 233$ K, $T_3 = 203$ K; – • – $T_2 = 193$ K, $T_3 = 223$ K.

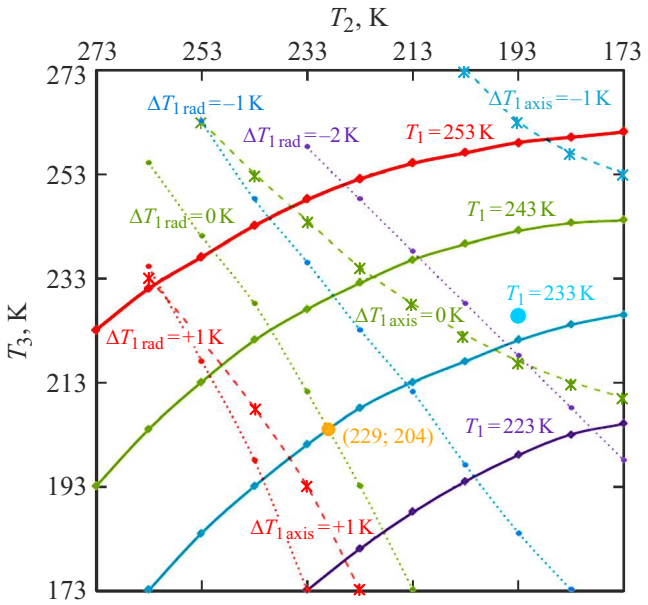

Figure 6. Nomogram of the distribution of the isotherms of the temperature state of the CPM depending on the temperature of the cryo-screens with $\varepsilon_4 = 0.57$.

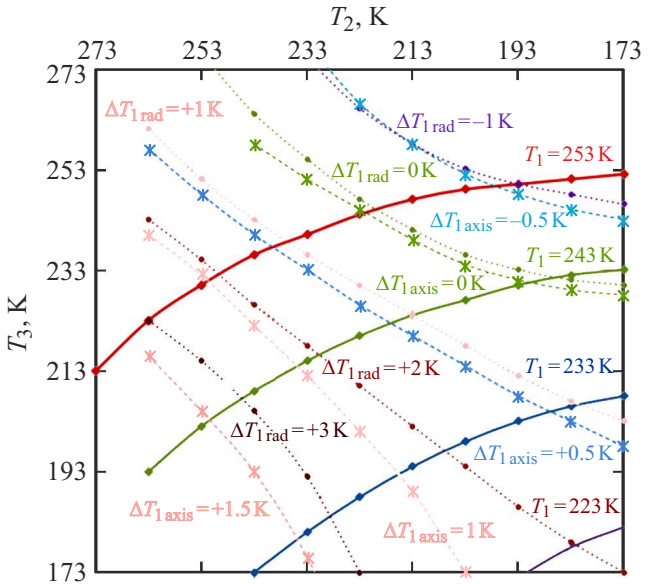

Figure 7. Nomogram of the distribution of the isotherms of the temperature state of the CPM as a function of the temperature of the cryo-screens in the absence of SVTI on cryo-screens and at $\varepsilon_4 = 0.1$.

cryo-screens. However, temperature gradients in this range will change both along the mirror axis (ΔT_{axis}) and along its radius (ΔT_{rad}). Therefore, the optimal cooling mode of the mirror is chosen such a mode in which these gradients are minimal. In particular, this condition corresponds to $T_2 = 229$ K and $T_3 = 204$ K for the temperature $T_1 = 233$ K (Fig. 6), i.e. zero radial temperature drop with an axial drop of less than 1 K.

It is obvious that a change in the structure of the thermostat will also lead to a change in the cooling modes of the CPM (Fig. 7). So, the required temperature values of cryo-screens are significantly reduced in the absence of SVTI and with the degree of blackness of the screen *4* $\varepsilon_4 = 0.1$ to ensure a thermal balance condition at $T_1 = 233$ K, namely T_3 decreases from 213 to 194 K at a constant $T_2 = 213$ K. At the same time, both axial and radial temperature differences in the mirror increase to 1–2 K.

The given nomograms illustrate the possibilities of the developed method for calculating the cooling modes of large-sized optics under vacuum conditions using various thermostat structures.

The impact of the presence of SVTI on the screen *4* and the degree of blackness of its inner surface on the radial temperature drop of the CPM is illustrated by the results of the analysis of nomograms given in Table 1 for the case of cooling of the CPM to $T_1 = 233$ K.

Table 1 shows that in the presence of SVTI and $\varepsilon_4 = 0.1$ (option 1), the difference between the temperatures of the screen *4* and the mirror is insignificant and amounts to $T_1 - T_4 = 0.5$ K, which ensures that there is practically no radial temperature drop of the mirror. In this case, the mirror temperature is higher than the screen temperature *4*, since the heat flow from the walls of the vacuum chamber *9* is limited by SVTI with high thermal resistance, and the screen *4* is actively cooled by cryo-screens. The degree of blackness $\varepsilon_4 = 0.1$ in the presence of SVTI contributes to the minimum temperature difference between the screen *4* and the mirror.

In the absence of SVTI and $\varepsilon_4 = 0.1$ (option 2), the difference $T_1 - T_4 = -18.2$ K, the screen temperature *4* is higher than the temperature of the CPM, since the heat flow from the walls of the vacuum chamber *9* increased compared to option 1, where SVTI is present on the screen *4*. At the same time, the radial difference in the mirror is greater than 4 K.

With a higher degree of blackness of the inner surface of the screen *4* $\varepsilon_4 = 0.57$ (option 3) and the presence of SVTI in the conditions of thermal balance of the system $T_1 - T_4 = -0.3$ K, which corresponds to zero radial temperature drop in the mirror. The temperature of the mirror in this case is slightly lower than the temperature of the screen *4*, since, having a higher degree of blackness compared to option 2, the inner surface of the screen *4* is cooled more strongly by cryo-screens.

The difference between the temperatures of the mirror and the screen *4* is $T_1 - T_4 = -4.7$ K in the absence of SVTI with the same degree of blackness of the inner surface of the screen *4* $\varepsilon_4 = 0.57$ (option 4). The temperature of the screen *4* is higher compared to option 3, since the heat flow from the walls of the chamber *9* through the screen *5* has increased due to the lack of SVTI.

It is important to note that in the absence of SVTI, it is possible to ensure the temperature of the mirror 233 K by setting lower values of the temperature of the cryo-screens than in the structure of the thermostat with the

Table 1. Conditions for the optimal thermal balance of the system in the cooling modes of the CPM to a temperature of $T_1 = 233$ K

A variant of the structure	SVTI	ε_4	T_2, K	T_3, K	ΔT_{axis}, K	ΔT_{rad}, K	$T_1 - T_4$, K
1	+	0.1	197	209	0.4	0	0.5
2	−	0.1	173	187	1.1	4.2	−18.2
3	+	0.57	229	204	0.8	0	−0.3
4	−	0.57	193	203	0.5	1.2	−4.7

Table 2. The conditions of the thermal balance of the system in the cooling modes of the CPM to the temperature $T_1 = 233$ K without cooling and with additional cooling of the stand

Option Designs of the stand T_8, K	Temperature	ε_4	T_2, K	T_3, K	ΔT_{axis}, K	$T_1 - T_4$, K
1	230.4*	0.1	−90	−90	1.0	−17.3
2	231.5*	0.57	−80	−69	0.5	−3.5
3	223**	0.1	−100	−58	0	1.2
4	223**	0.57	−60	−70	0.8	−4.5
5	203**	0.1	−80	−50	0	0.5
6	203**	0.57	−60	−60	0.5	−1.1

Note. * is the temperature of the stand under conditions of thermal equilibrium in the system; ** is the set temperature of the stand.

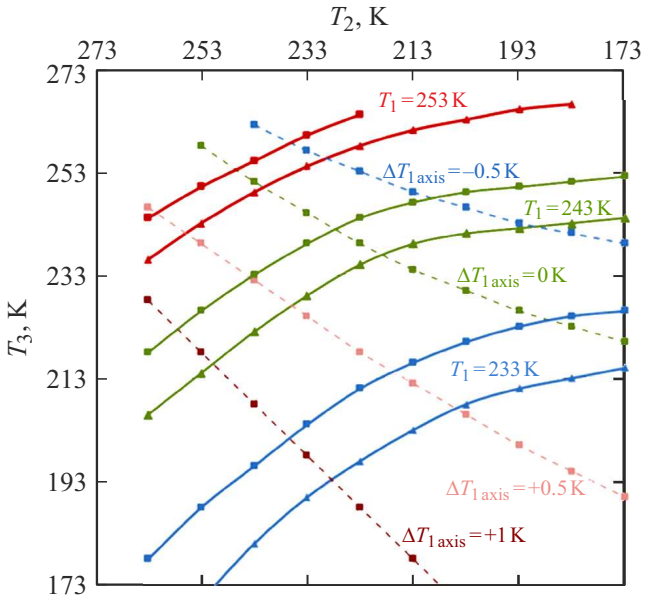

Figure 8. Nomogram of the thermostat structure without SVTI at $\varepsilon_4 = 0.57$: ▲ — $T_8 = 223$ K, ■ — $T_8 = 203$ K.

presence of SVTI. The effect of the degree of blackness of the screen *4* varies depending on the presence or absence of SVTI. $\varepsilon_4 = 0.57$ is preferable in the presence of SVTI, since the radial temperature drop in the mirror in this case is smaller and the temperature of the cryo-screens is higher. It is preferable to choose $\varepsilon_4 = 0.1$ in the absence of SVTI for the same reason.

The values of axial temperature differences in the CPM were within the tolerance in calculations of all variants of the thermostat structure. It should also be noted that at the same time the temperature of the mirror stand was always close to the temperature of the mirror in the conditions of the thermal balance of the thermostat and the CPM.

The cooling modes of the mirror at different values of the temperature of the stand were calculated to assess the effect of additional cooling of the stand based on the conditions of the thermal balance of the system „CPM−thermostat−vacuum chamber“. The results of calculations at the temperature of the stand $T_8 = 223$ and 203 K are shown below on the nomogram (Fig. 8). It is necessary to refer to the nomogram of the equilibrium states of this variant of the thermostat structure to analyze these results, but without additional cooling of the stand (Fig. 6).

The temperature of the stand was set to $T_8 = 230.4$ K (Table 2) in the absence of additional cooling of the stand in the conditions of thermal balance. Forced cooling of the stand to 223 K slightly reduced the load on the cryo-screens and now it is possible to cool the mirror to 233 K at higher temperatures of the cryo-screens T_2 and T_3. It is possible to achieve the same mirror temperature with even higher cryo-screen temperatures with the temperature of the stand $T_8 = 203$ K.

Thus, ensuring the optimal cooling mode of the optical elements in the thermostat significantly depends on the specific structure of the thermostat. The developed method of thermal calculation makes it possible to determine the possible range of changes of the cryo-screen temperature values, which provides minimum temperature gradients when the thermal deformations of the optics elements are within the calculated tolerance.

Conclusion

A method is proposed for calculating the cooling modes of large-sized optics based on a model of stationary thermal balance of a closed system of solids under vacuum conditions, provided by both radiation heat exchange and conductive heat transfer due to the thermal conductivity of the materials of the cooled elements. Conductive heat transfer is taken into account without involving non-stationary heat conduction equations, which significantly reduces the computing time and allows for a relatively fast optimization of both the structure of the thermostat and the cooling modes of the optics. At the same time, the cooling modes are controlled using cryo-screens, the temperature parameters of which can change independently of each other.

The determination of the optimal cooling mode of optical elements is reduced to finding such values of the cryo-screen temperature at which the mirror is cooled with minimal temperature gradients. It is shown that the representation of the results of thermal calculations in the form of nomograms of the temperature state of optical elements makes it possible to find such a range of changes in the temperature values of cryo-screens in which the temperature gradients that occur are minimal or within the optical tolerance.

The thermal balance method significantly accelerates the optimization of the solution of the multiparametric problem of cooling optical elements, depending on both the design and thermophysical parameters of the cooling system and optics.

The thermal balance method can also be used in other tasks of developing deep cooling systems for large-sized optics up to cryogenic temperatures, which will require taking into account changes in the thermophysical properties of optical materials.

Conflict of interest

The authors declare that they have no conflict of interest.

References

[1] L.S. Oleinikov. *Methody i sredstva stabilizatsii opticheskikh parametrov krioteleskopov kosmicheskogo bazirovaniya i nazemnykh imitatsionno-ispytatelnykh kompleksov*. Diss. d.t.n. (Spb, 2004)
[2] J.A. Clinea, J. Quenneville, R. Taylor, T.R. Deschenes, M. Braunstein, H. Legner, B.D. Green. Proc. SPIE, **8876**, 88760R (2013). DOI: 10.1117/12.2024371
[3] S.V. Kravchenko, S.B. Nesterov, V.A. Romanko, N.A. Testoedov, V.I. Halimanovich. Inzh. zhurn: nauka i innovatsii, **1** (13) (2013). DOI: 10.18698/2308-6033-2013-1-598
[4] I.Yu. Dmitriev, A.A. Kotmakova, Yu.A. Rezunkov. ZhTF, **91** (2), 213 (2021) (in Russian). DOI: 10.21883/TP.2023.05.56061.253-22
[5] ANSYS. Ed. by P. Kohnke, Ph.D. (Ansys Inc., 1994)
[6] R. Siegel, J. Howell. *Teploobmen izlucheniem* (Mir, M., 1975) (in Russian)
[7] V.N. Andrianov. *Osnovy radiatsionnogo i slozhnogo teploobmena* (Energia, M., 1972)
[8] G.A. Golitsin, A.P. Levich. Filosofskie nauki, **1**, 105 (2004) (in Russian).
[9] A.J. Bushman, Jr., C.M. Pittman. *Technical Note/ Langley Research Center/Langley Air Force Base/National Aeronautics and Space Administration* (Washington, 1961)

Translated by A.Akhtyamov